Acta of Bioengineering and Biomechanics
Vol. 13, No. 1, 2011

Original paper

Topology of calculating pressure and friction coefficients for time-dependent human hip joint lubrication

KRZYSZTOF WIERZCHOLSKI*

Pomeranian Academy of Słupsk, Institute of Applied Mathematics, Poland.

The paper deals with the calculations of the unsteady, impulsive pressure distributions, carrying capacities and friction forces under unsteady conditions in a super-thin layer of biological synovial fluid inside the slide biobearing gap limited by a spherical bone head. Unsteady and random flow conditions for the biobearing lubrication are given. Moreover, the numerical topology of pressure calculation for a difference method is applied. From a mathematical viewpoint the present method for the solution of the modified Reynolds equation allows this problem to be resolved by the partial recurrence nonhomogeneous equation of the second order with variable coefficients. To the best of the author knowledge, an adaptation of the known numerical difference method to the spherical boundary conditions applied during the pressure calculations for a human hip bonehead seems to be decisive.

Key words: *pressure, carrying capacity, unsteady conditions, new numerical difference method*

1. Introduction

The present paper deals with the latest achievements in calculation algorithm and the derivation of impulsive load carrying capacity distribution and friction coefficient of intelligent biopairs, especially for spherical, biobearing human hip joint surfaces. It is worth noticing that this paper is a natural continuation of author's scientific research [17]–[23].

We assume that spherical bone head in human hip joint moves at least in two directions: circumferential and meridian. Basic equations describing synovial fluid flow in human hip joint are solved in both analytical and numerical ways. The numerical calculations are performed in Mathcad 12 Professional Program, with taking into account the method of recurrence solutions. Partial differential equations of the motion in lubrication theory are simulated by the partial recurrence equations. This method satisfies the stability conditions of numerical solutions of partial differential equations and gives real values of fluid velocity components and friction forces in human hip joints.

2. Basic equations

Many lubrication theories for diarthrodial hip joints have been proposed, but a theoretical model of friction coefficient determination for impulsive and periodic lubrication of human joint has not been completely formulated: [1], [3]–[6], [12], [13]. Comparison between periodic viscoelastic lubrication and impulsive one of human joint was not considered in [8], [10], [11], [14], [15]–[17]. In this paper, the kind of lubrication occurs near two co-operating hip joint surfaces suddenly set in motion after an impulse. Synovial fluid has non-Newtonian properties according to DOWSON's investigations [1]. The Rivlin–Ericksen constitutive equations presented in [23] have been used for the description of such a fluid. Bone head of both sound and pathological joints has often ellipsoidal shape, but

* Corresponding author: Krzysztof Wierzcholski, Institute of Applied Mathematics, Pomeranian University of Słupsk, ul. Arciszewskiego, 76-200 Słupsk, Poland. Phone: +48 59 840 53 28, fax: +48 59 840 54 75, e-mail: krzysztof.wierzcholski@wp.pl

Received: May 23rd, 2010
Accepted for publication: August 30th, 2010

the difference between its semi-minor and semi-major axes cannot be greater than the minimum value of gap height to make the rotary motion possible [1]. Thus, we can assume a spherical shape of bone head. Spherical bone head can be put into rotary motion in one or two different directions (figure 1).

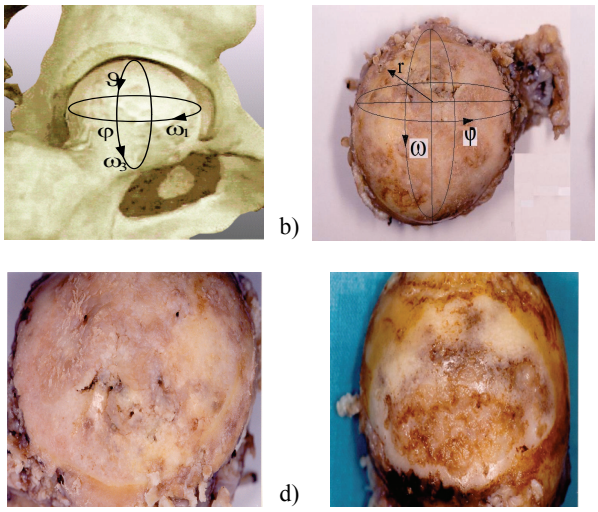

Fig. 1. Human hip joint: sound spherical bone head (a), pathological bone heads (b), (c), (d)
φ – coordinate in the circumferential direction,
r – coordinate in the gap-height direction,
ϑ – coordinate in the meridional direction

For synovial fluid flow in joint gap, three-dimensional components v_φ, v_r, v_ϑ of velocity in three directions φ, r, ϑ are considered. The symbols v_φ, v_r, v_ϑ denote synovial fluid velocity components in the circumferential, gap-height and meridional directions of bone head, respectively. The pressure p depends on the variables φ, ϑ and the time t. The gap height ε may be the function of three variables, i.e., φ, ϑ and t. The basic equations [23] describing synovial fluid flow in the gap of a human joint during impulsive and unsteady motion of human limbs are solved in a semi-analytical way and a new-numerical way. The numerical calculations are performed in Mathcad 12 Professional Program, with taking into account the recurrence equation method. This method satisfies the stability conditions of numerical solutions of partial differential equations and gives the real values of load carrying capacity and friction coefficients in human hip joints. The problem of impulsive, unsteady lubrication of a human hip joint will be solved for the joint surfaces between bone head and acetabulum by means of the equations of conservation of momentum and continuity equation [8], [9], [18], [23]:

$$\text{Div}\,\mathbf{S} = \rho\mathbf{a}, \qquad \text{Div}\,\mathbf{v} = 0,$$

$$\mathbf{S} = -p\mathbf{I} + \eta\mathbf{A}_1 + \alpha\mathbf{A}_1^2 + \beta\mathbf{A}_2, \tag{1}$$

where:

$\mathbf{S}$ – the stress tensor,

p – the pressure,

$\mathbf{I}$ – the unit tensor,

$\mathbf{A}_1$ and $\mathbf{A}_2$ – the first two Rivlin–Ericksen tensors,

η, α, β – three material constants; $\eta = \eta_0\eta$ is a dynamic viscosity in Pas, α, β are pseudo-viscosity coefficients in Pas^2,

ρ – the synovial fluid density in kg/m^3.

The tensors $\mathbf{A}_1$ and $\mathbf{A}_2$ are given by symmetric matrices [8], [9], [18]:

$$\mathbf{A}_1 \equiv \mathbf{L} + \mathbf{L}^T, \quad \mathbf{A}_2 \equiv \text{grad}\,\mathbf{a} + (\text{grad}\,\mathbf{a})^T + 2\mathbf{L}^T\mathbf{L},$$
$$\mathbf{a} \equiv \mathbf{L}\,\mathbf{v} + \frac{\partial \mathbf{v}}{\partial t}, \tag{2}$$

where:

$\mathbf{L}$ – the tensor of fluid velocity gradient vector in s^{-1},

$\mathbf{L}^T$ – the tensor for transpose of a matrix of gradient vector of a synovial fluid in s^{-1},

$\mathbf{v}$ – the velocity vector in m/s,

t – the time in s,

$\mathbf{a}$ – the acceleration vector in m/s^2.

According to the experimental research [1], the lubrication and pressure distribution region spreads in the circumferential direction from angle $\varphi = 0$ to the half perimeter of spherical bone, i.e., $\varphi = \pi$. In the meridional direction, the pressure generation begins at the angle $\vartheta_1 = \pi/8$ (i.e., about 22 grades distant from the upper pole of spherical bone head) and spreads to the remaining part of the upper hemisphere up to the angle $\vartheta_1 = \pi/2$. Hence, the lubrication region is defined as follows: $0 \le \varphi \le 2\pi\theta_1$, $0 < \theta_1 < 1$, $\pi R/8 \le \vartheta \le \pi R/2$, $0 \le r \le \varepsilon$, $\vartheta_1 = \vartheta/R$, ε is the gap height. The terms multiplied by the coefficient β denote the influence of the time-variable viscoelastic properties of synovial fluid on the hip joint lubrication.

3. Impulsive lubrication

3.1. Method of solutions

Impulsive perturbations start at the origin of the time interval. The impulsive perturbations of lubrication parameters decrease with the time t. If the time t tends to infinity, then the perturbations tend to zero and we have the classical lubrication of human hip

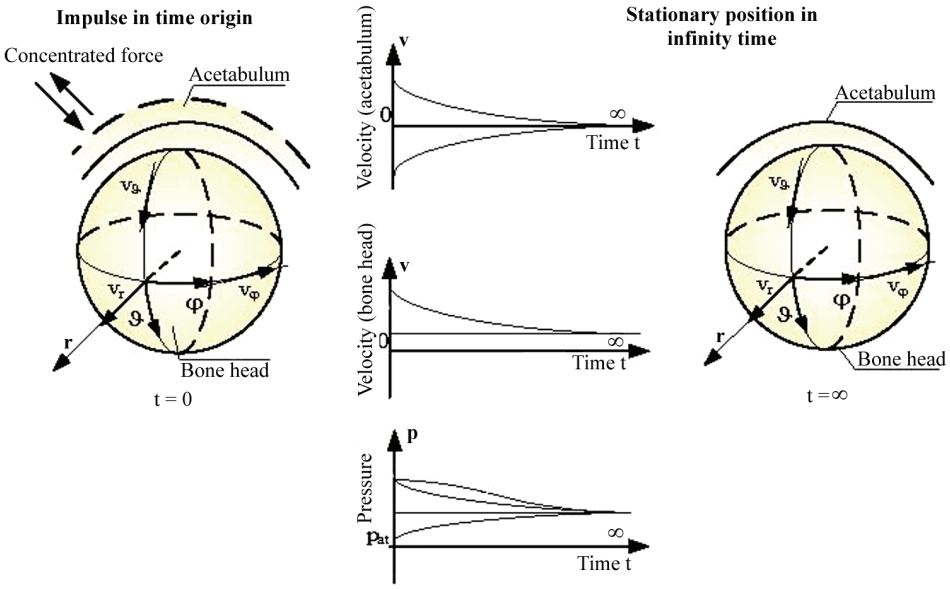

Fig. 2. Flow and lubrication parameters for human hip joint in impulsive, unsteady motion

joint with synovial fluid of Newtonian properties. The lubrication and flow parameters varying with time for impulsive motion are presented in figure 2.

In order to solve the system of equations (1)–(2), one introduces a solution using expansion by power function series. Assuming successive powers of the function $\beta/(\eta_0 t)$, we obtain finally [2], [18]:

$$
\begin{aligned}
v_\varphi &= U\left[v_{\varphi 0}(\chi,\varphi,\vartheta_1) + \frac{\beta}{\eta_0 t} v_{\varphi 1}(\chi,\varphi,\vartheta_1) \right. \\
&\left. + \left(\frac{\beta}{\eta_0 t}\right)^2 v_{\varphi 2}(\chi,\varphi,\vartheta_1) + \ldots \right], \\
v_\vartheta &= U\left[v_{\vartheta 0}(\chi,\varphi,\vartheta_1) + \frac{\beta}{\eta_0 t} v_{\vartheta 1}(\chi,\varphi,\vartheta_1) \right. \\
&\left. + \left(\frac{\beta}{\eta_0 t}\right)^2 v_{\vartheta 2}(\chi,\varphi,\vartheta_1) + \ldots \right], \\
v_r &= U\psi\left[v_{r0}(\chi,\varphi,\vartheta_1) + \frac{\beta}{\eta_0 t} v_{r1}(\chi,\varphi,\vartheta_1) \right. \\
&\left. + \left(\frac{\beta}{\eta_0 t}\right)^2 v_{r2}(\chi,\varphi,\vartheta_1) + \ldots \right], \\
p &= \frac{UR\eta_0}{\varepsilon_0^2}\left[p_{10}(\varphi,\vartheta_1,t_1) + \frac{\beta}{\eta_0 t} p_{11}(\varphi,\vartheta_1,t_1) \right. \\
&\left. + \left(\frac{\beta}{\eta_0 t}\right)^2 p_{12}(\varphi,\vartheta_1,t_1) + \ldots \right]
\end{aligned}
\tag{3}
$$

with

$$
\begin{gathered}
\chi \equiv \frac{r}{2\sqrt{\nu t}} = r_1 N_\varepsilon, \quad N_\varepsilon \equiv \frac{\varepsilon_0}{2\sqrt{\nu t}}, \quad \nu \equiv \frac{\eta_0}{\rho}, \\
t > 0, \quad 0 < \frac{\beta}{\eta_0 t} < 1, \quad 0 < r_1 < \varepsilon_1, \quad r = \varepsilon_0 r_1.
\end{gathered}
\tag{4}
$$

The synovial fluid velocity components of $v_{\varphi k}$, $v_{\vartheta k}$, v_{rk} and the pressure p_{1k} for $k = 0$ depend on the time and synovial fluid dynamic viscosity, but they are independent of its viscoelastic properties. Flow parameters for $k = 1, 2, \ldots$ describe the corrections of synovial fluid velocity components and the pressure caused by the time-dependent viscoelastic properties of synovial fluid. The functions $v_{\varphi k}$, $v_{\vartheta k}$, p_{1k} and the quantities χ, N_ε are dimensionless. By inserting the expressions (3)–(4) into the system of equations (1), (2), we arrive at the following ordinary differential equations for the first six unknown functions $v_{\varphi 0}$, $v_{\vartheta 0}$, $v_{\varphi 1}$, $v_{\vartheta 1}$, $v_{\varphi 2}$, $v_{\vartheta 2}$:

$$
\begin{aligned}
&\frac{d^2 v_{\varphi 0}}{d\chi^2} + 2\chi \frac{dv_{\varphi 0}}{d\chi} = \frac{4\nu t}{\varepsilon_0^2 \sin(\vartheta_1)} \frac{\partial p_{10}}{\partial \varphi}, \\
&\frac{d^2 v_{\vartheta 0}}{d\chi^2} + 2\chi \frac{dv_{\vartheta 0}}{d\chi} = \frac{4\nu t}{\varepsilon_0^2} \frac{\partial p_{10}}{\partial \vartheta_1}, \\
&\frac{d^2 v_{\varphi 1}}{d\chi^2} + 2\chi \frac{dv_{\varphi 1}}{d\chi} + 4v_{\varphi 1} \\
&= \frac{4\nu t}{\varepsilon_0^2 \sin(\vartheta_1)} \frac{\partial p_{11}}{\partial \varphi} + \frac{d^2 v_{\varphi 0}}{d\chi^2} + \frac{1}{2}\chi \frac{d^3 v_{\varphi 0}}{d\chi^3},
\end{aligned}
\tag{5}
$$

$$\frac{d^2 v_{\vartheta 1}}{d\chi^2} + 2\chi \frac{dv_{\vartheta 1}}{d\chi} + 4v_{\vartheta 1}$$

$$= \frac{4\nu t}{\varepsilon_0^2} \frac{\partial p_{11}}{\partial \vartheta_1} + \frac{d^2 v_{\vartheta 0}}{d\chi^2} + \frac{1}{2}\chi \frac{d^3 v_{\vartheta 0}}{d\chi^3}, \qquad (6)$$

$$\frac{d^2 v_{\varphi 2}}{d\chi^2} + 2\chi \frac{dv_{\varphi 2}}{d\chi} + 8v_{\varphi 2}$$

$$= \frac{4\nu t}{\varepsilon_0^2 \sin(\vartheta_1)} \frac{\partial p_{12}}{\partial \varphi} + 2\frac{d^2 v_{\varphi 1}}{d\chi^2} + \frac{1}{2}\chi \frac{d^3 v_{\varphi 1}}{d\chi^3},$$

$$\frac{d^2 v_{\vartheta 2}}{d\chi^2} + 2\chi \frac{dv_{\vartheta 2}}{d\chi} + 8v_{\vartheta 2}$$

$$= \frac{4\nu t}{\varepsilon_0^2} \frac{\partial p_{12}}{\partial \vartheta_1} + 2\frac{d^2 v_{\vartheta 1}}{d\chi^2} + \frac{1}{2}\chi \frac{d^3 v_{\vartheta 1}}{d\chi^3}, \qquad (7)$$

……,

where:

$0 \le \chi \equiv r_1 N_\varepsilon < \varepsilon_1 N_\varepsilon$,
$0 < r_1 < \varepsilon_1$,
$0 < \varphi < 2\pi$,
$\pi R/8 \le \vartheta \le \pi R/2$,
$\vartheta_1 = \vartheta/R$.

3.2. Boundary conditions and particular solutions

The spherical bone head moves in the circumferential direction φ only. Hence, the synovial fluid velocity components on the bone head surface in the circumferential direction equal the peripheral velocity of spherical surface of bone head. These velocity values are changing in the meridional direction ϑ according to the variations of the function sin(*). The peripheral velocity in the circumferential direction on the pole of bone head equals zero for $\vartheta_1 = 0$, and on the equator of spherical bone has a dimensionless value of unity for $\vartheta_1 = \pi/2$. The synovial fluid velocity component on spherical bone head surface in the meridional direction ϑ equals zero, because the spherical bone head is motionless in the direction ϑ.

Viscous synovial fluid flows around the bone head. Hence, on the bone head surface the synovial fluid velocity component in the gap-height direction equals zero.

The spherical acetabulum surface is motionless in the circumferential and meridional directions. Thus, the synovial fluid velocity components on the acetabulum surface are equal to zero in the circumferential and meridional directions. But the spherical bone head does not sustain any changes in gap-height direction. Hence the gap height changes with time. Therefore the synovial fluid velocity component in the gap-height direction r equals the first derivative of the gap height with respect to the time.

The corrections of the values of the synovial fluid velocity components cannot change the boundary conditions presented above which are assumed on the bone head and acetabulum surface in the circumferential, meridional and gap-height directions. Therefore, for the synovial fluid velocity components and their corrections we have the following boundary conditions:

$$r = 0, \quad \chi = 0, \quad v_{\varphi 0} = \sin\vartheta_1,$$
$$v_{\varphi 1} = 0,..., \quad v_{\varphi k} = 0,..., \qquad (8)$$
$$r = 0, \quad \chi = 0, \quad v_{\vartheta 0} = 0,$$
$$v_{\vartheta 1} = 0,..., \quad v_{\vartheta k} = 0, ...,$$
$$r = 0, \quad \chi = 0, \quad v_{r0} = 0,$$
$$v_{r1} = 0,..., \quad v_{rk} = 0,...,$$
$$r = \varepsilon, \quad \chi = N_\varepsilon \varepsilon_1, \quad v_{\varphi 0} = 0,$$
$$v_{\varphi 1} = 0,..., \quad v_{\varphi k} = 0,..., \qquad (9)$$
$$r = \varepsilon, \quad \chi = N_\varepsilon \varepsilon_1, \quad v_{\vartheta 0} = 0,$$
$$v_{\vartheta 1} = 0,..., \quad v_{\vartheta k} = 0,...,$$
$$r = \varepsilon, \quad \chi = N_\varepsilon \varepsilon_1, \quad v_{r0} = St\,\partial\varepsilon_1/\partial t_1,$$
$$v_{r1} = 0,..., \quad v_{rk} = 0,...$$

with $St \equiv 1/\omega_0 t_0$, $t_1 = t/t_0$ and $k = 1, 2, 3,...$

For $\beta = 0$ one obtains the equation for the original Reynolds problem.

The boundary conditions for the velocity components in unsteady Newtonian and non-Newtonian flows in impulsive motion are presented in figure 3.

Solutions of the equations (5), (7) have been found in closed form. Imposing the boundary conditions (8), (9) on the general solutions of the differential equations (5), (7),we obtain finally the following particular solutions:

$$v_{\varphi 0}(\varphi, r_1, \vartheta_1, t_1) = +\sin\vartheta_1$$

$$-\left\{\sin\vartheta_1 - \frac{\sqrt{\pi}}{2N_\varepsilon^2 \sin\vartheta_1} \frac{\partial p_{10}}{\partial \varphi} Y_0(\chi = N_\varepsilon \varepsilon_1)\right\}$$

$$\times \frac{\operatorname{erf}(r_1 N_\varepsilon)}{\operatorname{erf}(\varepsilon_1 N_\varepsilon)} - \frac{\sqrt{\pi}}{2N_\varepsilon^2 \sin\vartheta_1} \frac{\partial p_{10}}{\partial \varphi} Y_0(\chi = N_\varepsilon r_1), \qquad (10)$$

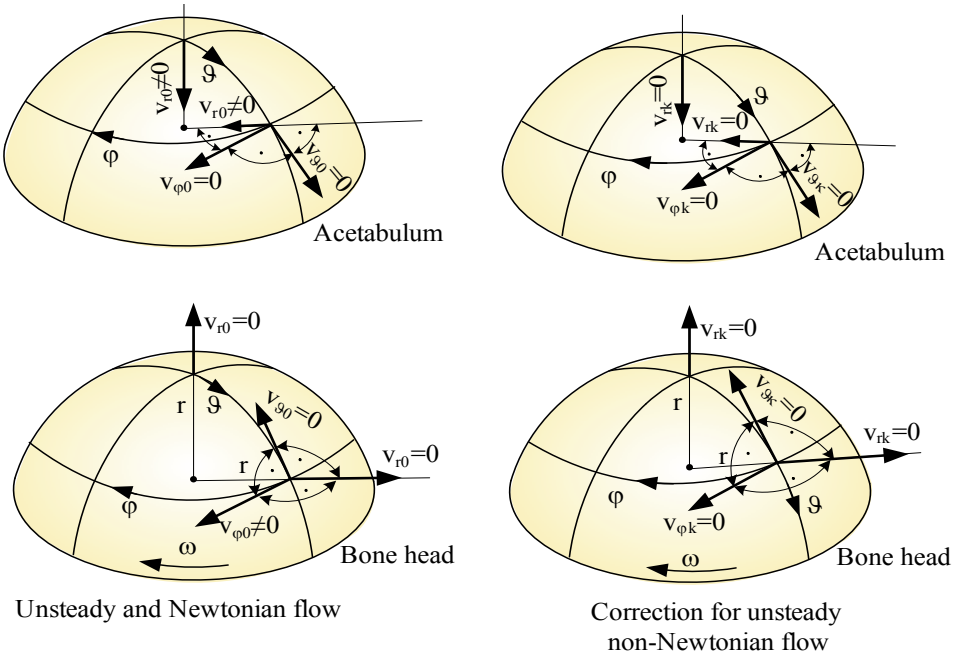

Fig. 3. Boundary conditions for velocity components on the bone head and acetabulum in impulsive unsteady Newtonian flow and corrections caused by the unsteady non-Newtonian flow for impulsive motion

$$v_{\vartheta 0}(\varphi, r_1, \vartheta_1, t_1) = \frac{\sqrt{\pi}}{2N_\varepsilon^2}\frac{\partial p_{10}}{\partial \vartheta_1} Y_0(\chi = N_\varepsilon \varepsilon_1)$$

$$\times \frac{\operatorname{erf}(r_1 N_\varepsilon)}{\operatorname{erf}(\varepsilon_1 N_\varepsilon)} - \frac{\sqrt{\pi}}{2N_\varepsilon^2}\frac{\partial p_{10}}{\partial \vartheta_1} Y_0(\chi = N_\varepsilon r_1) \qquad (11)$$

with

$$Y_0(\chi) \equiv \int_0^{\chi_y} e^{\chi_1^2} \operatorname{erf}\chi_1 d\chi_1 - \operatorname{erf}\chi \int_0^{\chi} e^{\chi_1^2} d\chi_1,$$
$$\operatorname{erf}\chi_1 \equiv \frac{2}{\sqrt{\pi}} \int_0^{\chi_1} \exp(-\chi_2^2) d\chi_2, \qquad (12)$$

and $0 \le t_1 < \infty$, $0 \le r_1 \le \varepsilon_1$, $b_{m1} \le \vartheta_1 \le b_{s1}$, $0 < \varphi < 2\pi\theta_1$, $0 \le \theta_1 < \infty$, $0 \le \chi_2 \le \chi_1 \le \chi \equiv r_1 N_\varepsilon \le \varepsilon_1 N_\varepsilon$, $\varepsilon_1 = \varepsilon_1(\varphi, \vartheta_1)$.

The synovial fluid velocity components in the circumferential and meridional directions for unsteady Newtonian fluid being in impulsive motion have the forms of (10), (11).

The corrections of the values of the synovial fluid velocity components caused by the unsteady conditions and viscoelastic non-Newtonian properties of the fluid being in impulsive motion in circumferential and meridional directions are obtained from equations (6), (7).

We put the series (3) into the continuity equation [23] and equate the terms multiplied by the first powers of the coefficient $\beta/(\eta_0 t_0)$ which is of small value. Hence, we obtain the following equation:

$$\frac{\partial v_{\varphi 0}}{\partial \varphi} + \sin(\vartheta / R)\frac{\partial v_{r0}}{\partial r_1}$$

$$+ \frac{\partial}{\partial \vartheta_1}[v_{\vartheta 0} \sin(\vartheta / R)] = 0\,. \qquad (13)$$

Integrating equation (13) with respect to r_1 and imposing the boundary conditions $(8)_3$ on the synovial fluid velocity component and its corrections in the gap-height direction we arrive at [18]:

$$v_{r0}(\varphi, \vartheta_1, r_1, t_1) = -\frac{1}{\sin\vartheta_1}\frac{\partial}{\partial\varphi}\int_0^{r_1} v_{\varphi 0} dr_1$$

$$-\frac{1}{\sin\vartheta_1}\frac{\partial}{\partial\vartheta_1}\int_0^{r_1} (\sin\vartheta_1) v_{\vartheta 0} dr_1. \qquad (14)$$

The synovial fluid velocity component in the gap-height direction for unsteady but Newtonian fluid, being in impulsive motion, is represented by (14). Imposing the boundary conditions $(9)_3$ on the velocity components (14) and inserting solution (11) into equation (14), we obtain the following modified Reynolds equation [18]:

$$\frac{\sqrt{\pi}}{2N_\varepsilon^2}\frac{1}{\sin\vartheta_1}\frac{\partial}{\partial\varphi}\left\{\left[\frac{\int_0^{\varepsilon_1}\operatorname{erf}(r_1N_\varepsilon)dr_1}{\operatorname{erf}(\varepsilon_1N_\varepsilon)}Y_0(\chi=N_\varepsilon\varepsilon_1)-\int_0^{\varepsilon_1}Y_0(\chi=N_\varepsilon r_1)dr_1\right]\frac{\partial p_{10}}{\partial\varphi}\right\}$$

$$+\frac{\sqrt{\pi}}{2N_\varepsilon^2}\frac{\partial}{\partial\vartheta_1}\left\{\left[\frac{\int_0^{\varepsilon_1}\operatorname{erf}(r_1N_\varepsilon)dr_1}{\operatorname{erf}(\varepsilon_1N_\varepsilon)}Y_0(\chi=N_\varepsilon\varepsilon_1)-\int_0^{\varepsilon_1}Y_0(\chi=N_\varepsilon r_1)dr_1\right]\frac{\partial p_{10}}{\partial\vartheta_1}\sin\vartheta_1\right\}$$

$$=-(\sin\vartheta_1)\frac{\partial}{\partial\varphi}\left(\int_0^{\varepsilon_1}\left[1-\frac{\operatorname{erf}(r_1N_\varepsilon)}{\operatorname{erf}(\varepsilon_1N_\varepsilon)}\right]dr_1\right)-St\frac{\partial\varepsilon_1}{\partial t_1}\sin\vartheta_1, \tag{15a}$$

$0 \le r_2 \le r_1 \le \varepsilon_1$, $0 \le \varphi < 2\pi\theta_1$, $0 \le \theta_1 < 1$, $0 \le \vartheta_1 < \pi/2$, $0 \le t_1 < \infty$, $0 \le \chi_1 \le \chi \le \varepsilon_1 N_\varepsilon$.

The pressure corrections, i.e., p_{11},..., caused by the non-Newtonian oil properties are made based on equations (6), (7). The modified Reynolds equation (15a) represents the unknown function $p_{10}(\varphi, \vartheta_1, t_1)$. If t_1 tends to infinity, i.e. $N_\varepsilon \to 0$, $St \to 0$, then equation (15a) tends to the classical Reynolds equation:

$$\frac{1}{\sin\vartheta_1}\frac{\partial}{\partial\varphi}\left(\varepsilon_1^3\frac{\partial p_{10}}{\partial\varphi}\right)+\frac{\partial}{\partial\vartheta_1}\left(\varepsilon_1^3\frac{\partial p_{10}}{\partial\vartheta_1}\sin\vartheta_1\right)$$

$$=6\frac{\partial\varepsilon_1}{\partial\varphi}\sin\vartheta_1. \tag{15b}$$

The time-dependent gap height with perturbations has the following form [18]:

$$\varepsilon(\phi,\vartheta,t)=\varepsilon_0\varepsilon_1(\phi,\vartheta_1,t_1)$$

$$=\varepsilon^{(0)}[1+s_1\exp(-t_0t_1\omega_0)],$$

$$\varepsilon^{(0)}\equiv\varepsilon_\Delta-R+[(\varepsilon_\Delta)^2$$

$$+(R+\varepsilon_{\min})(R+2D+\varepsilon_{\min})]^{0.5}, \tag{16}$$

$$\varepsilon_\Delta\equiv\Delta\varepsilon_x\cos\phi\sin\vartheta_1$$

$$+\Delta\varepsilon_y\sin\phi\sin\vartheta_1-\Delta\varepsilon_z\cos\vartheta_1.$$

In the time-dependent gap height, we transform coordinates from the rectangular (x, y, z) into the spherical (φ, r, ϑ) for $\vartheta_1 = \vartheta/R$. We take into account the centre of spherical bone head O(0, 0, 0) and the centre of spherical acetabulum $O_1(x - \Delta\varepsilon_x, y - \Delta\varepsilon_y, z + \Delta\varepsilon_z)$.

The concentrated force [18] acts on the spherical surface of hyper-elastic acetabulum and generates the cartilage and gap-height deformations $s(\varphi, \vartheta)$ in the radial direction. The longer the time up to the impulse, the smaller the deformations multiplied by s_1 according to the exponential function. The coefficient s_1 describes the dimensionless changes of gap height caused by an impulsive load during the motion. The gap height increases if $s_1 > 0$ and decreases if $s_1 < 0$. The greater the concentrated force of impulse, the greater the absolute value of the coefficient s_1. The symbol ω_0 denotes an angular velocity or frequency in s^{-1} and describes the changes of time-dependent perturbations in synovial fluid impulsive flow in joint gap in its height direction.

If t_1 tends to infinity, then the gap height (16) tends to the time-independent gap height for stationary flow. We assume the centre of spherical bone head in the point $O(0, 0, 0)$ and the centre of spherical acetabulum in the point $O_1(x - \Delta\varepsilon_x, y - \Delta\varepsilon_y, z + \Delta\varepsilon_z)$. Eccentricity has the value D.

The lubrication region for impulsive motion and time-dependent gap-height changes in impulsive motion is denoted by Ω: $0 \le \varphi \le \pi$, $\pi R/8 \le \vartheta \le \pi R/2$. It is a section of the bowl of the sphere. The pressure p_{10} distributed along the boundary of the region is equal to the atmospheric pressure p_{at}. The pressure corrections p_{11}, p_{12},... on the boundary of the region equal zero.

The final dimensional form of the pressure distribution for unsteady impulsive motion and viscoelastic properties of synovial fluid is as follows:

$$p = \frac{\omega R^2 \eta_0}{\varepsilon_0^2}\left[p_{10}(\varphi, \vartheta_1, t_1) + \frac{\beta}{\eta_0 t} p_{11}(\varphi, \vartheta_1, t_1) + \mathrm{O}\left(\frac{\beta}{\eta_0 t}\right)^2 \right], \tag{17}$$

where the dimensionless pressure function p_{10} is determined from equation (15a).

3.3. Friction coefficients in spherical coordinates

Friction coefficients in spherical coordinates are as follows [21]:

$$\mu_{\mathrm{sph}} = \frac{\sqrt{F_{R\varphi}^2(t) + F_{R\vartheta}^2(t)}}{C_{\mathrm{tot}}^{(\mathrm{sph})}}, \tag{18}$$

where the symbol $C_{\mathrm{tot}}^{(\mathrm{sph})}$ stands for the load-carrying capacity in spherical hip joint defined in [23], and $F_{R\varphi}$, $F_{R\vartheta}$ are the time-dependent friction forces in two perpendicular directions φ and ϑ in spherical coordinates.

4. Results of numerical calculations

The topology of the recurrence method of solutions is presented in Appendix. In impulsive motion, the dimensionless pressure p_{10} and its dimensionless corrections p_{11}, p_{12},... are determined in the lubrication region Ω by virtue of the modified Reynolds equations (15a), (A18), taking into account the gap height (17). The time-dependent friction force coefficients are calculated by virtue of the equations derived (18).

Numerical calculations are performed in Matlab 7.2 Professional Program for the following parameters: the radius of spherical bone head $R = 0.0265$ m, the angular velocity or frequency of impulsive perturbations of the gap height at the Strouhal number $St = 125000$ and the characteristic dimensional time $t_0 = 0.00001$ s.

The gap height (16) is taken into account, and the following eccentricities of bone head $\Delta\varepsilon_x = 4.0$ μm, $\Delta\varepsilon_y = 0.5$ μm, $\Delta\varepsilon_z = 3$ μm have been assumed. The method of finite differences is applied [7].

From DOWSON's experiment [1] it follows that the dynamic viscosity η_0 of synovial fluid reaches 0.40 Pas, and from the theory of viscoelastic fluids [1], [9] it can be deduced that the pseudoviscosity coefficient β equals 0.000001 Pas^2. Moreover, we assume the density of synovial fluid $\rho = 1010$ kg/m^3, the angular velocity of spherical bone head $\omega = 0.8$ s^{-1}, and the average minimum gap height $\varepsilon_{\min}$ which changes at the time interval of 0.00001 s $\le t \le$ 100 s and attains the values from 3.8 μm to 5.8 μm. The average relative radial clearance $\psi \equiv \varepsilon/R = 3.774 \cdot 10^{-4}$, the Strouhal number $St = 125000$, $Re \cdot \psi \cdot St = 0.025$, $De \cdot St = 0.250$. In this case, we have $0 \le \beta/\eta_0 t < 1$. For the dimensionless times values: $t_1 = 1$, $t_1 = 10^2$, $t_1 = 10^4$, $t_1 = 10^6$, $t_1 = 10^7$, $t_1 = 10^8$, i.e., for the dimensional time values: $t = 0.00001$ s; $t = 0.001$ s; $t = 0.1$ s; $t = 10.0$ s; $t = 100.0$ s; t = 1000.0 s, respectively, and for $s_1 = \pm 0.20$ we obtain the pressure distributions shown in figures 4 and 5, and the maximum pressure and capacity distributions – in figure 6.

To obtain real values of time, we multiply the dimensionless values t_1 by the characteristic time value $t_0 = 0.00001$ s. For example, $t_1 = 100\,000$ denotes 1 s after an impulse. The time scale presented enables us to determine important pressure changes occurring within some microseconds after injury.

The pressure distributions shown on the right-hand side of figures 4 and 5 are obtained for an increasing of gap height caused by impulsive effects. In this case, if the time after the impulse increases, the gap height decreases, hence the pressure increases. The pressure distributions on the left-hand side of figures 4 and 5 are obtained for the decreasing of gap height caused by impulsive effects. In this case, if the time after the impulse increases, the gap height increases, hence the pressure decreases.

If the time is long enough after the impulse, i.e. for $t_1 \to \infty$, the pressure distributions for the increasing ($s_1 > 0$) and decreasing ($s_1 < 0$) effects of gap-height changes caused by the impulse tend to identical pressure distributions (see figures 5 and 6). This limit pressure distribution can also be obtained from the classical Reynolds equation (15b).

By virtue of calculations presented in this paper it can be concluded that in human hip joint, for fixed time, the total friction force, carrying capacity and friction coefficient increase if angular velocity and dynamic viscosity of synovial fluid increase (see figures 7, 8, 9).

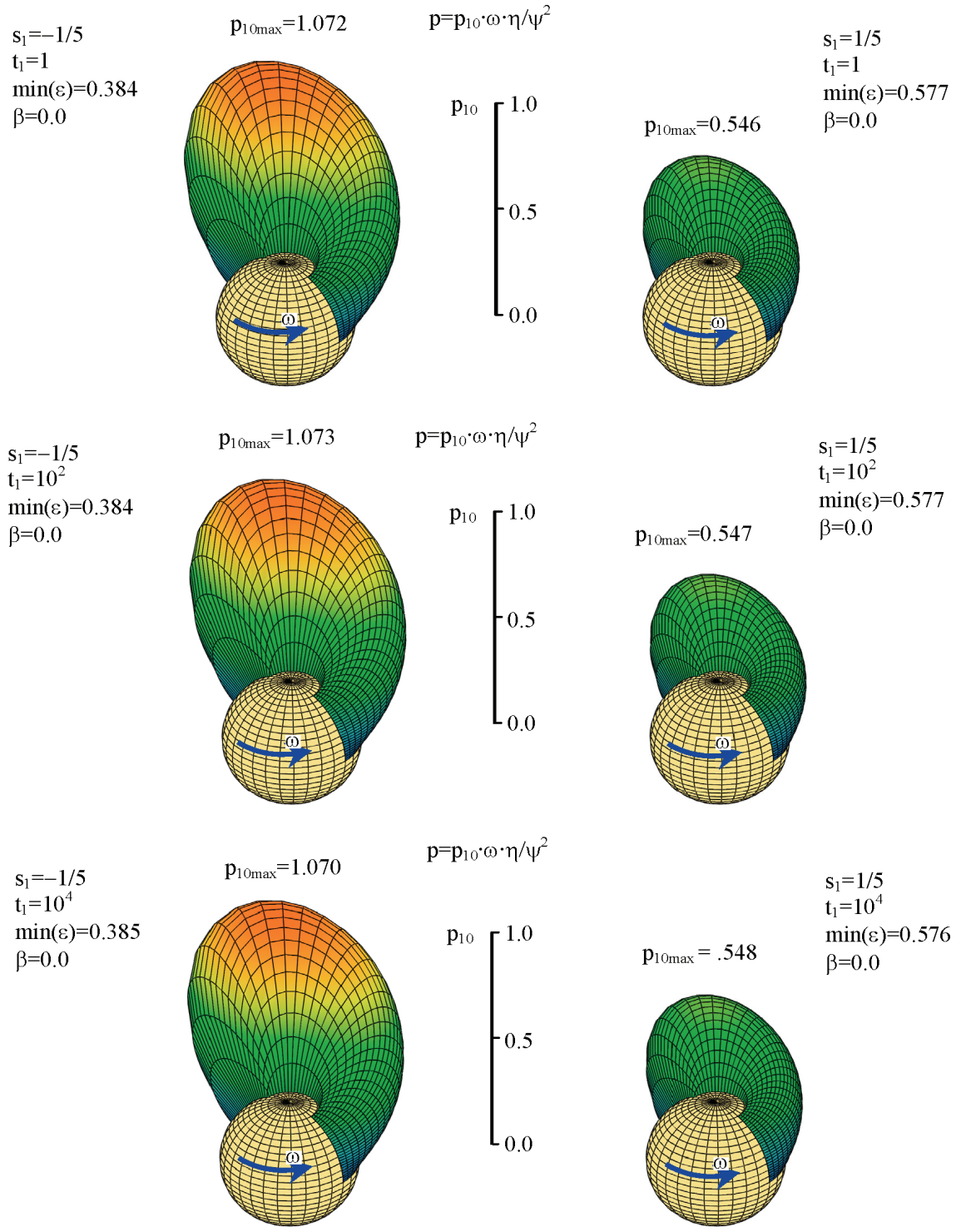

Fig. 4. Dimensionless hydrodynamic pressure distributions inside the gap of human spherical hip joint in the region Ω: $0 \le \varphi \le \pi$, $\pi R/8 \le \vartheta \le \pi R/2$ for the dimensionless time values: $t_1 = 1$ (i.e., $t = 0.00001$ s), $t_1 = 100$ (i.e., $t = 0.001$ s), $t_1 = 10000$ (i.e., $t = 0.1$ s), after the impulse moment for the increasing (decreasing) effects of gap-height changes see the right (left) column of figures, respectively. The results are obtained for the following data: $R = 0.0265$ m; $\eta_0 = 0.40$ Pas; $\rho = 1010$ kg/m^3; $\Delta\varepsilon_x = 4$ μm; $\Delta\varepsilon_y = 0.5$ μm; $\Delta\varepsilon_z = 3$ μm; $\psi \equiv \varepsilon/R \approx 3.774 \cdot 10^{-4}$; $\omega = 0.8$ s^{-1}; $St = 125000$; $Re \cdot \psi \cdot St = 0.025$; $De \cdot St = 0.250$

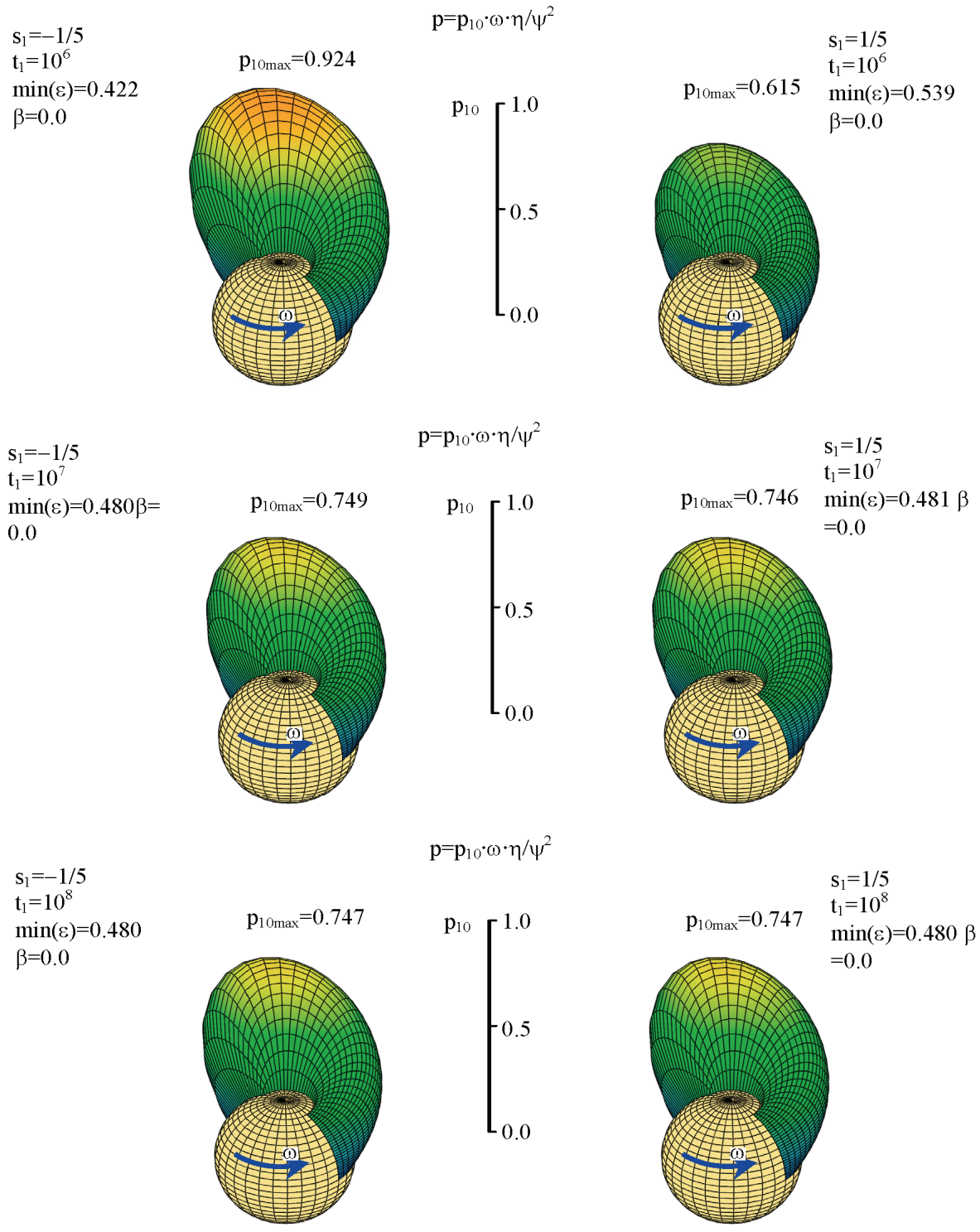

Fig. 5. Dimensionless hydrodynamic pressure distributions inside the gap of human spherical hip joint in the region Ω: $0 \le \varphi \le \pi$, $\pi R/8 \le \vartheta \le \pi R/2$ for the dimensionless time values: $t_1 = 10^6$, (i.e., $t = 10$ s), $t_1 = 10^7$ (i.e., $t = 100$ s), $t_1 = 10^8$ (i.e., $t = 1000$ s), after the impulse moment for the increasing (decreasing) effects of gap height changes see the right (left) column of figures, respectively. The results are obtained for the following data: $R = 0.0265$ m; $\eta_0 = 0.40$ Pas; $\rho = 1010$ kg/m^3; $\Delta\varepsilon_x = 4$ μm; $\Delta\varepsilon_y = 0.5$ μm; $\Delta\varepsilon_z = 3$ μm; $\omega = 0.8$ s^{-1}; $\psi \equiv \varepsilon/R \approx 3.774 \cdot 10^{-4}$; $St = 125000$; $Re \cdot \psi \cdot St = 0.025$; $De \cdot St = 0.250$

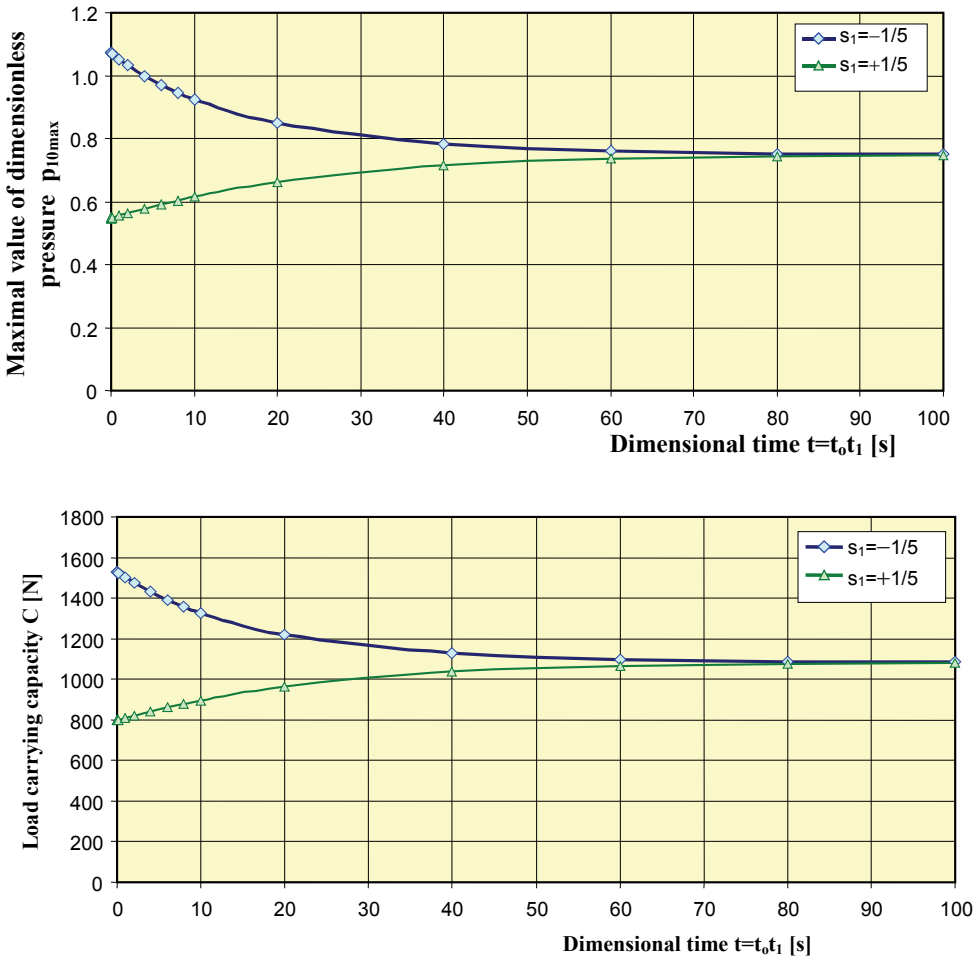

Fig. 6. Maximum dimensionless hydrodynamic pressure values inside the gap of slide spherical biobearing and dimensional capacity values in the region Ω: $0 \le \varphi \le \pi$, $\pi R/8 \le \vartheta \le \pi R/2$ versus the dimensional time interval from $t = 0.00001$ s to $t = 100$ s, after the impulse moment, calculated for the following data: $R = 0.0265$ m; $\eta_0 = 0.40$ Pas; $\rho = 1010$ kg/m^3; $\Delta\varepsilon_x = 4$ μm; $\Delta\varepsilon_y = 0.5$ μm; $\Delta\varepsilon_z = 3$ μm; $\psi \equiv \varepsilon/R \approx 3.774 \cdot 10^{-4}$; $\omega = 0.8$ s^{-1}; $St = 125000$; $Re \cdot \psi \cdot St = 0.025$; $De \cdot St = 0.250$. The upper (lower) curve of the presented numerical values refers to the decreasing (increasing) effects of gap-height changes after the impulse moment

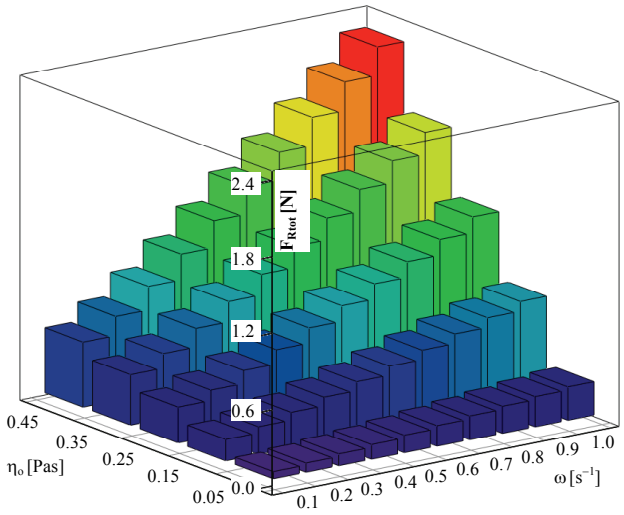

Fig. 7. Total values of friction forces in human spherical hip joint versus angular velocity of bone head and dynamic viscosity of synovial fluid

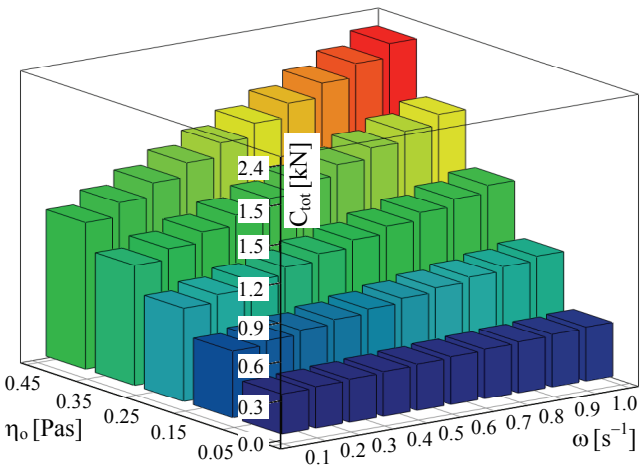

Fig. 8. The carrying capacity values in human hip joint versus the bone head angular velocity and synovial fluid dynamic viscosity

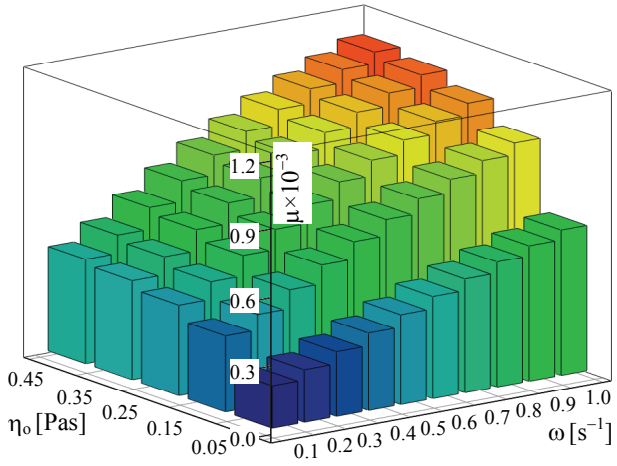

Fig. 9. The friction coefficients in human hip joint versus the bone head angular velocity and synovial fluid dynamic viscosity during human walk

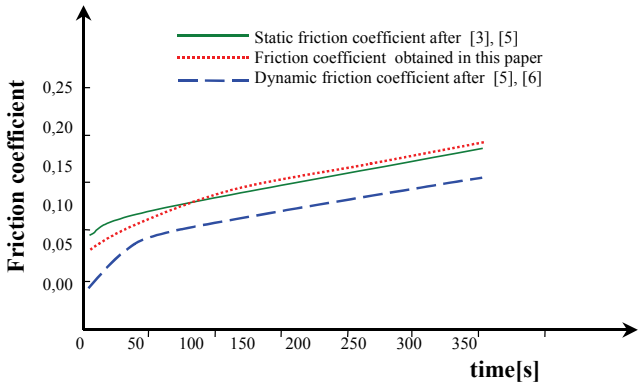

Fig. 10.Time-dependent friction coefficient values calculated by the author and the results obtained in [3], [5], [6] for long time periods

In recently published papers [21], [22], the author derived the formulas for time-dependent velocity components and pressure distributions in curvilinear coordinates. The results obtained previously [22] are now used to formulae the time-dependent friction forces and time-dependent friction coefficients based on equations (26), (27), (28). The results for long and short time intervals are presented in figures 10 and 11.

5. Conclusions

The present paper shows the analytical and numerical calculations of the velocities, hydrodynamic pressure and friction coefficients of synovial fluid in the gap of spherical human hip joint during impulsive motion.

- It has been proved that in long time periods, the friction coefficient decreases.
- The numerical calculations of pressure, carrying capacity and friction force distributions after injury are carried out with full details, taking into account the perturbations of the gap of human hip joint, resulting from impulsive motion.
- The influence of the viscoelastic time-dependent properties of synovial fluid on the pressure and friction forces distributions in human hip joint is presented.
- A new form of the modified Reynolds equation obtained tends, in this particular case, towards the

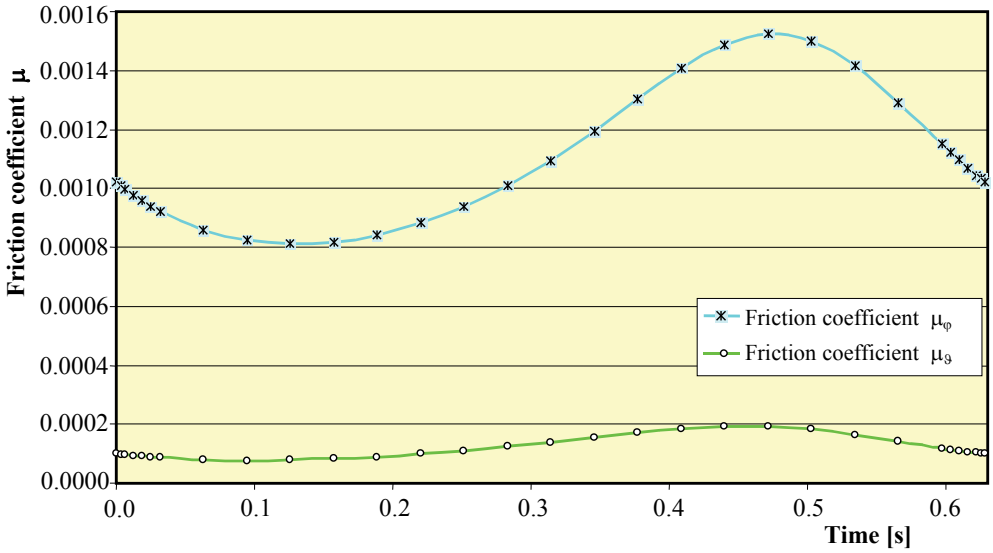

Fig. 11. The total friction coefficients in circumferential φ and meridional ϑ directions of spherical human hip joint versus dimensional time presented in decimal scale for perturbations connected with human walk in short time periods

well-known form of Reynolds equation for steady motion, which was derived in preceding papers. We have demonstrated that the total apparent viscosity of synovial fluid depends on the velocity deformations and time.

Acknowledgements

This paper was supported by the BW/10/9025826/09 founds. Moreover, the author thanks for the financial help of Polish Ministerial Grant 3475/B/T02/2009/36 in years 2009–2012.

Appendix: topology of recurrence method of solutions

The Reynolds equation (15a) can be written in the following form:

$$E(\vartheta_1)\frac{\partial}{\partial\varphi}\left[A(\varphi,\vartheta_1,t_1)\frac{\partial p_{10}}{\partial\varphi}\right] + F\frac{\partial}{\partial\vartheta_1}\left[B(\varphi,\vartheta_1,t_1)\frac{\partial p_{10}}{\partial\vartheta_1}\right] = G(\vartheta_1)\frac{\partial H(\varphi,\vartheta_1,t_1)}{\partial\varphi} + J(\varphi,\vartheta_1,t_1). \tag{A1a}$$

After transformations the modified Reynolds equation (A1a) takes the following form

$$E\frac{\partial A}{\partial\varphi}\frac{\partial p_{10}}{\partial\varphi} + EA\frac{\partial^2 p_{10}}{\partial\varphi^2} + \frac{\partial B}{\partial\vartheta_1}\frac{\partial p_{10}}{\partial\vartheta_1} + B\frac{\partial^2 p_{10}}{\partial\vartheta_1^2} = G\frac{\partial H}{\partial\varphi} + J. \tag{A1b}$$

We seek for the solution of the unknown dimensionless pressure p_{10} from equation (A1b), taking into account progressive differences in the difference method and recurrence equations in lubrication region domain Ω: $0 \le \varphi \le 2\pi\theta$, $0 < \theta < 1$, $\pi/8 \le \vartheta_1 \le \pi/2$, $\vartheta_1 = \vartheta/R$. Subintervals in the direction φ are described by the index i and subintervals in the directions ϑ_1 are denoted by the index j. The division of region domain is defined as follows:

$$\Omega(\varphi_i,\vartheta_{1j}):\begin{cases} i=1,2,3,...,M, \\ j=1,2,3,...,N. \end{cases} \tag{A2a}$$

The steps of division of the region domain Ω are as follows:

$$h \equiv \varphi_{i+1}-\varphi_i, \quad k \equiv \vartheta_{1j+1}-\vartheta_{1j}$$

$$\text{for} \quad i=1,2,...,M; \quad j=1,2,...,N. \tag{A2b}$$

Spherical region Ω contains NM nodes, where $2M + 2N - 4$ nodes are on the boundary of the region and $NM - 2(N + M) + 4$ are internal nodes. Figure A1 shows the region Ω and one node.

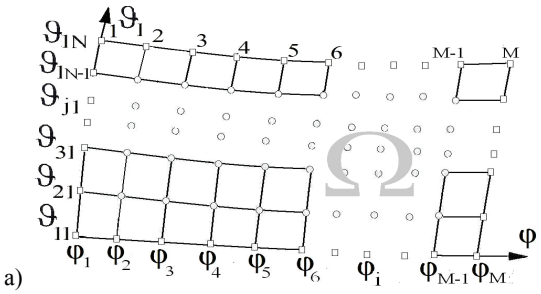

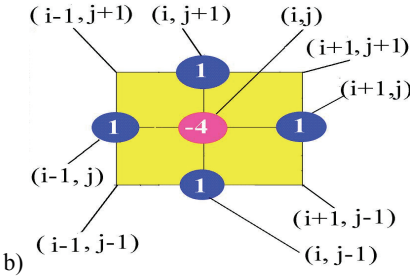

Fig. A1. The domain Ω of the lubrication region (a), calculation node (b)

The values of the functions A, B, E, G, H, J in the nodes of divided region Ω for $i = 1, 2,...,M - 1, M$; $j = 1, 2,...,N - 1, N$ we denote by the following formulae:

$$A[\varepsilon_1(\varphi=\varphi_i,\vartheta_1=\vartheta_{1i},t_1)] = A(\varepsilon_{i,j}) = A_{i,j}, \tag{A3}$$

$$B[\varepsilon_1(\varphi=\varphi_i,\vartheta_1=\vartheta_{1i},t_1)\vartheta_1=\vartheta_{1i}] = A_{i,j}\sin\vartheta_j = B_{i,j}, \tag{A4}$$

$$E(\vartheta_1=\vartheta_{1i}) = E_j = \operatorname{cosec}(\vartheta_j), \tag{A5}$$

$$G(\vartheta_1=\vartheta_{1i}) = G_j = -\frac{\varepsilon_0^2\cdot\rho}{2\sqrt{\pi}\,\eta_0 t_0}\sin(\vartheta_j), \tag{A6}$$

$$H[\varepsilon_1(\varphi=\varphi_i,\vartheta_1=\vartheta_{1i},t_1)] = H(\varepsilon_{i,j}) = H_{i,j}, \tag{A7}$$

$$J[\varepsilon_1(\varphi=\varphi_i,\vartheta_1=\vartheta_{1i},t_1),\vartheta_1=\vartheta_{1i}] = J_{i,j} = \left(\frac{\varepsilon^{(0)}}{\varepsilon_0}\right)_{i,j} s_1\exp(-t_1/St), \tag{A8}$$

$$p_{10}[\varphi=\varphi_i,\vartheta_1=\vartheta_{1i},t_1]=p_{i,j}, \tag{A9}$$

$$\varepsilon_1[\varphi=\varphi_i,\vartheta_1=\vartheta_{1i},t_1]=\varepsilon_{i,j}$$

$$=\left(\frac{\varepsilon^{(0)}}{\varepsilon_0}\right)_{i,j}[1+s_1\exp(-t_1/St)], \tag{A10}$$

$$\left(\frac{\varepsilon^{(0)}}{\varepsilon_0}\right)_{i,j}\equiv\{\varepsilon_{\Delta i,j}-R+[(\varepsilon_{\Delta i,j})^2 + (R+\varepsilon_{\min})(R+2D+\varepsilon_{\min})]^{0.5}\}\varepsilon_0^{-1}, \tag{A11}$$

$$\varepsilon_{\Delta i,j}\equiv\Delta\varepsilon_x\cos\varphi_i\sin\vartheta_j + \Delta\varepsilon_y\sin\varphi_i\sin\vartheta_j-\Delta\varepsilon_z\cos\vartheta_j.$$

The pressure function $p(\varphi,\ \vartheta_1)$ is expanded into Taylor series in the neighborhood of the point $(\varphi+h,\ \vartheta+k)$ as follows:

$$p(\varphi+h,\vartheta+k)=p(\varphi,\vartheta)+\left(h\frac{\partial}{\partial\varphi}+k\frac{\partial}{\partial\vartheta}\right)p(\varphi,\vartheta)+\frac{1}{2!}\left(h\frac{\partial}{\partial\varphi}+k\frac{\partial}{\partial\vartheta}\right)^2 p(\varphi,\vartheta)+\ldots+\frac{1}{n!}\left(h\frac{\partial}{\partial\varphi}+k\frac{\partial}{\partial\vartheta}\right)^n \times p(\varphi+\Theta_\varphi h,\vartheta+\Theta_\vartheta k), \tag{A12a}$$

where $0<\Theta_\varphi,\ \Theta_\vartheta<1$.

From expansion (A12a) the function $p(\varphi,\ \vartheta_1)$ in the neighborhood of the point (i, j) has the form:

$$p_{i+h,j+k}=p_{ij}+h(p_\varphi)_{ij}+k(p_\vartheta)_{ij}+0.5\,h^2(p_{\varphi\varphi})_{ij}+hk(p_{\varphi\vartheta})_{ij}+0.5\,k^2(p_{\vartheta\vartheta})_{ij}+O(h^3)+O(k^3). \tag{A12b}$$

From (A12b) it follows:

$$0.5\ \{h^2p_{\varphi\varphi}+k^2p_{\vartheta\vartheta}\}_{ij}=p_{i+h,j+k}-p_{ij}-h(p_\varphi)_{ij}-k(p_\vartheta)_{ij}-hk(p_{\varphi\vartheta})_{ij}+O(h^3)+O(k^3). \tag{A13}$$

We insert $h = 1$, $k = 0$ and $h = –1$, $k = 0$ into formula (A13) and multiply both sides of the equation by EA. If we sum up the equations obtained, we arrive at:

$$EA\frac{\partial^2 p}{\partial\alpha_1^2}=\frac{E_{i,j}A_{i,j}}{h^2}p_{i+1,j}+\frac{E_{i,j}A_{i,j}}{h^2}p_{i-1,j}-2\frac{E_{i,j}A_{i,j}}{h^2}p_{i,j}. \tag{A14}$$

We insert $h = 0$, $k = 1$ and $h = 0$, $k = –1$ into formula (A13) and multiply both sides of equation by FB. If we sum up the equations obtained, we arrive at:

$$FB\frac{\partial^2 p}{\partial\alpha_3^2}=\frac{F_{i,j}B_{i,j}}{k^2}p_{i,j+1}+\frac{F_{i,j}B_{i,j}}{k^2}p_{i,j-1}-2\frac{F_{i,j}B_{i,j}}{k^2}p_{i,j}. \tag{A15}$$

We take into account the following differences:

$$\left(\frac{\partial A}{\partial\varphi}\right)_i\left(\frac{\partial p}{\partial\varphi}\right)_i\approx p_{i+1,j}\frac{A_{i+1,j}-A_{i,j}}{h^2}-p_{i,j}\frac{A_{i+1,j}-A_{i,j}}{h^2}, \tag{A16}$$

$$\left(\frac{\partial B}{\partial\vartheta}\right)_j\left(\frac{\partial p}{\partial\vartheta}\right)_j\approx p_{i,j+1}\frac{B_{i,j+1}-B_{i,j}}{k^2}-p_{i,j}\frac{B_{i,j+1}-B_{i,j}}{k^2}. \tag{A17}$$

If we insert (A14)–(A17) into equation (A1b) and if we take into account $F = 1$ and formulae (A3)–(A11), then for each node presented in figure A1b we obtain the following partial recurrence equation:

$$\kappa_{i+1,j}p_{i+1,j}+\nu_{i,j+1}p_{i,j+1}+\pi_{i,j-1}p_{i,j-1}+\xi_{i-1,j}p_{i-1,j}-Z_{i,j}p_{i,j}=Q_{i,j}+J_{i,j}\equiv Q^*_{i,j}, \tag{A18}$$

where for $i = 1, 2,...,M – 1$, M; $j = 1, 2,...,N –1$ we have:

$$\kappa_{i+1,j}\equiv\frac{A_{i+1,j}}{h^2}\operatorname{cosec}(\vartheta_j),\qquad \nu_{i,j+1}\equiv\frac{B_{i,j+1}}{k^2}=\frac{A_{i,j+1}}{k^2}\sin(\vartheta_j), \tag{A19}$$

$$\pi_{i-1,j}\equiv\frac{A_{i,j}}{h^2}\operatorname{cosec}(\vartheta_j), \tag{A20}$$

$$\xi_{i,j-1} \equiv \frac{B_{i,j}}{k^2} = \frac{A_{i,j}}{k^2}\sin(\vartheta_j), \tag{A20}$$

$$Z_{i,j} \equiv \frac{A_{i+1,j} + A_{i,j}}{h^2}\operatorname{cosec}(\vartheta_j) + \frac{A_{i,j+1} + A_{i,j}}{k^2}\sin(\vartheta_j), \tag{A21}$$

$$Q^*_{i,j} \equiv J_{i,j} + G_{i,j}\frac{H_{i+1,j} - H_{i,j}}{h} = \left(\frac{\varepsilon^{(0)}}{\varepsilon_0}\right)_{i,j} s_1 \exp(-t_1/St) = -\frac{\varepsilon_0^2 \cdot \rho}{2\sqrt{\pi}\, h\eta_0 t_0}\sin(\vartheta_j) \times \left(\int_0^{\varepsilon_{i+1,j}} \left[1 - \frac{\operatorname{erf}(r_1 N_\varepsilon)}{\operatorname{erf}(\varepsilon_1 N_\varepsilon)}\right] dr_1 - \int_0^{\varepsilon_{i,j}} \left[1 - \frac{\operatorname{erf}(r_1 N_\varepsilon)}{\operatorname{erf}(\varepsilon_1 N_\varepsilon)}\right] dr_1 \right). \tag{A22}$$

By virtue of (15a), (A1a) + (A3) we can write the following discrete form of the function A:

$$A_{i,j} \equiv \int_0^{\varepsilon_{i,j}} \operatorname{erf}(r_1 N_\varepsilon)\, dr_1 \times \left(\frac{\int_0^{\varepsilon_{i,j} N_\varepsilon} \exp(\chi^2)\operatorname{erf}(\chi) d\chi}{\operatorname{erf}(r_1 N_\varepsilon)} - \int_0^{\varepsilon_{i,j} N_\varepsilon} \exp(\chi^2) d\chi \right) - \int_0^{\varepsilon_{i,j}} \left[\int_0^{r_1 N_\varepsilon} \exp(\chi^2)\operatorname{erf}(\chi) d\chi - \operatorname{erf}(r_1 N_\varepsilon) \int_0^{r_1 N_\varepsilon} \exp(\chi^2) d\chi \right] dr_1. \tag{A23}$$

The sequence of pressure values $\{p_{i,j}\}$ is unknown; however, the coefficients $\pi_{i,j} \equiv \pi_{ij}, \kappa_{i,j} \equiv \kappa_{ij}, \xi_{i,j} \equiv \xi_{ij}$, ... and the function $Q^*_{i,j}$ are known. If we take into account the same number of steps in the directions φ and ϑ_1, i.e., $M = N$, then the region $\Omega(\varphi, \vartheta_1)$ presented in figure A1 has $(N-2)^2$ internal nodes (i, j) for $i = 2,...,N-1$; $j = 2,...,N-1$. If we insert the index values i and j of each internal node into equation (A18), then we obtain the system of $(N-2)^2$ algebraic, linear, non-homogeneous equations with $(N-2)^2$ unknowns. For $4N-4$ boundary nodes of the region $\Omega(\phi, \vartheta_1)$ we impose the following boundary conditions:

$$\begin{aligned} (p_{10})_{1,j} &= 0 \quad \text{for} \quad j = 2, 3,..., N-1, \\ (p_{10})_{M,j} &= 0 \quad \text{for} \quad j = 2, 3,..., N-1, \\ (p_{10})_{i,1} &= 0 \quad \text{for} \quad i = 1, 2, 3,..., M, \\ (p_{10})_{i,N} &= 0 \quad \text{for} \quad i = 1, 2, 3,..., M. \end{aligned} \tag{A24}$$

The value of pressure differs from that of atmospheric one on the boundary line determined by the coordinate $\varphi = \varphi_M$, i.e., $i = M$ on the right side of the region $\Omega(\phi, \vartheta_1)$, see $(A24)_2$. Atmospheric values (≅zero values) are attained on the unknown curve of film end $\varphi^{(k)}_{i,j}$ which is restricted by the region $\Omega(\phi, \vartheta_1)$ from the right side. The region $\Omega(\phi, \vartheta_1)$ in the direction φ is restricted by the inequalities:

$$0 \le \varphi \le \varphi^{(k)}_{i,j}, \quad 0 \le \vartheta_1 \le \pi/2. \tag{A25}$$

An unknown coordinate of the film end $\varphi^{(k)}_{i,j}$ is determined from the Reynolds condition which has the following discrete form:

$$\frac{p_{i+1,j} - p_{i,j}}{h} = 0. \tag{A26}$$

The pressure surface in each point $(\vartheta_1)_j$,... for $i = M + \Delta_2, M + \Delta_3,...$ of the curve $\varphi^{(k)}_{i,j}$ is tangential to the region $\Omega(\varphi, \vartheta_1)$. We assume $N = M = 100$ steps in the dimensionless region $\Omega(\varphi, \vartheta_1)$: $0 \le \varphi \le \pi$; $\pi/8 \le \vartheta_1 \le \pi/2$. Hence, the length of the step in each direction is as follows: $h = \pi/100$, $k = 3\pi/800$. We insert such values into (A19)–(A23), hence we obtain the simplified form of the above equations, because $\varepsilon_0^2 \cdot \rho/(2\sqrt{\pi}\, h\eta_0 t_0) = 0.2267$ and $N_\varepsilon = 7.945 \cdot 10^{-3}$.

The coordinates (i, j) or (φ_i, ϑ_j), where $i = 2,...,99$, $j = 2,...,99$, for $98 \times 98 = 9604$ internal nodes of the region $\Omega(\varphi, \vartheta_1)$, presented in figure A1 for $N = M = 100$, are inserted into recurrence equation (A18) and then the boundary conditions (A24), (A26) are considered. We obtain the system of 9604 algebraic linear equations, determining 9604 unknown pressure values $(p_{10})_{ij}$.

A quadratic matrix **U** with 9604 rows and columns is presented as the matrix with 98 rows and 98 columns, where each element denotes minor, and each minor has 98 rows and 98 columns and is defined in the following form:

$$\mathbf{U}=\begin{bmatrix}
\mathbf{M}_2 & \mathbf{E}_{\nu 3} & \mathbf{O} & \mathbf{O} & \ldots & . & \mathbf{O} & \mathbf{O} & \mathbf{O} \\
\mathbf{E}_{\pi 2} & \mathbf{M}_3 & \mathbf{E}_{\nu 4} & \mathbf{O} & \ldots & . & \mathbf{O} & \mathbf{O} & \mathbf{O} \\
\mathbf{O} & \mathbf{E}_{\pi 3} & \mathbf{M}_4 & \mathbf{E}_{\nu 5} & . & . & \mathbf{O} & \mathbf{O} & \mathbf{O} \\
\mathbf{O} & \mathbf{O} & \mathbf{E}_{\pi 4} & \mathbf{M}_5 & . & . & \mathbf{O} & \mathbf{O} & \mathbf{O} \\
. & . & . & . & . & . & . & . & . \\
. & . & . & . & . & . & . & . & . \\
\mathbf{O} & \mathbf{O} & \mathbf{O} & \mathbf{O} & . & . & \mathbf{M}_{97} & \mathbf{E}_{\nu 98} & \mathbf{O} \\
\mathbf{O} & \mathbf{O} & \mathbf{O} & \mathbf{O} & . & . & \mathbf{E}_{\pi 97} & \mathbf{M}_{98} & \mathbf{E}_{\nu 99} \\
\mathbf{O} & \mathbf{O} & \mathbf{O} & \mathbf{O} & . & . & \mathbf{O} & \mathbf{E}_{\pi 98} & \mathbf{M}_{99}
\end{bmatrix}. \tag{A27}$$

Here the following sub-matrixes (minors) can be itemized:

i) $N^2 - 7N + 12 = 9312$ zero square sub-matrixes **O**: $(N-2)\times(N-2) = (98\times 98)$, each has 98 rows and 98 columns,

ii) $2N - 6 = 194$ unit square diagonal sub-matrixes $\mathbf{E}_{\pi s}$, $\mathbf{E}_{\nu m}$: $(N-2)\times(N-2) = (98\times 98)$, for $s = 2, 3, 4, 5, 6,\ldots,97, 98$; $m = 3, 4, 5,\ldots,98, 99$.The terms: π_{2s}, π_{3s}, $\pi_{4s},\ldots,\pi_{98s}$, π_{99s}, and ν_{2m}, ν_{3m}, ν_{4m}, $\nu_{5m},\ldots,\nu_{98m}$, ν_{99m} create the main diagonals of the matrixes mentioned,

iii) $N - 2 = 98$ three diagonal $\mathbf{M}_j$ sub-matrixes, $N - 2 = 98$, each has 98 rows and 98 columns and is presented in the three-diagonal form:

The unknown pressure values are obtained from the formula:

$$p_{i,j} = \frac{\det \mathbf{U}_{ij}}{\det \mathbf{U}} \tag{A30}$$

for $i, j = 2, 3, 3, 5$.

If we replace the column with the term $\mu_{i,j} = \mu_{5,3}$ in the matrix **U** with the column of free terms $[Q_{ij}]$, then the matrix $\mathbf{U}_{ij} = \mathbf{U}_{53}$ is accepted as true. It is: $i - 1 + (N-2)\cdot(j-2) = 5 - 1 + (100-2)(3-2) = 102$, i.e., the hundredth second column in the square matrix of 9604 rows and 9604 columns.

$$\mathbf{M}_j=\begin{bmatrix}
\mu_{2j} & \kappa_{3j} & 0 & 0 & . & , & 0 & 0 & 0 \\
\xi_{2j} & \mu_{3j} & \kappa_{4j} & 0 & . & . & 0 & 0 & 0 \\
0 & \xi_{3j} & \mu_{4j} & \kappa_{5j} & . & . & 0 & 0 & 0 \\
0 & 0 & \xi_{4j} & \mu_{5j} & . & . & 0 & 0 & 0 \\
. & . & . & . & . & . & . & . & . \\
. & . & . & . & . & . & . & . & . \\
0. & 0 & 0 & 0 & . & . & \mu_{97j} & \kappa & 0 \\
0 & 0 & 0 & 0 & . & . & \xi_{97j} & \mu_{98j} & \kappa_{99j} \\
0 & 0 & 0 & 0 & . & . & 0 & \xi_{98j} & \mu_{99j}
\end{bmatrix}, \tag{A28}$$

$j = 2, 3, 4, 5, 6, 7, 8,\ldots,N-1$; hence $j = 2, 3,\ldots,98, 99$.

The coefficients $\mu_{i,j}$ are calculated from the formula:

$$\mu_{ij} \equiv -Z_{i,j} = -\kappa_{i+1,j} + \nu_{i,j+1} + \pi_{i,j-1} + \xi_{i-1,j}. \tag{A29}$$

References

[1] DOWSON D., *Bio-Tribology of Natural and Replacement Synovial Joints*, [in:] Van Mow C., Ratcliffe A., Woo S.L-Y., *Biomechanics of Diarthrodial Joint*, Springer-Verlag, New York–Berlin–London–Paris–Tokyo–Hong Kong, 1990, Vol. 2, Chap. 29, 305–345.

[2] KNOPP K., *Szeregi nieskończone*, PWN, Warszawa, 1956.
[3] MERKHER Y., SIVAN S., ETSION I., MAROUDAS A., HALPERINA G., YOSEF A., *Rational human joint friction test*, Tribological Letter, 2006, 22(1), 29–36.
[4] MOW V.C, RATCLIFFE A., WOO S., *Biomechanics of Diarthrodial Joints*, Springer-Verlag, Berlin–Heidelberg–New York, 1990.
[5] NAKA M. H., HASUO M., FUWA Y., IKEUCHI K., *Correlation between friction of articular cartilage and reflectance intensity from superficial image*, Tribology International, 2007, 40(2), 200–207.
[6] NORTHWOOD E., FISHER J., *A multi-directional in vitro investigation into friction coefficient of articular cartilage depends on the contact area*, Journal of Biomechanics, 2007, 40, 3257–3260.
[7] RALSTON A., *A First Course in Numerical Analysis*, McGraw-Hill Co., New York–Toronto–London–Sydney, 1965.
[8] TEIPEL I., *The impulsive motion of a flat plate in a viscoelastic fluid*, Springer-Verlag, Acta Mechanica, 1981, 39, 277–279.
[9] TRUESDELL C.A., *First Course in Rational Continuum Mechanics*, Maryland, John Hopkins University, Baltimore, 1972.
[10] UNGETHÜM M., WINKLER-GNIEWEK W., *Tribologie in Medizin,* Tribologie Schmierungstechnik, 1990, 5, 268–277.
[11] WIERZCHOLSKI K., PYTKO S., *Metoda wyznaczania parametrów biołożyska smarowanego cieczą nienewtonowską*, Tribologia, 1993, 1, 9–12.
[12] WIERZCHOLSKI K., PYTKO S., *Analytical calculations for experimental dependences between shear rate and synovial fluid viscosity*, Proc. of Internat. Tribology Conference, Japan, Yokohama, 1995, Vol. 3, 1975–1980.
[13] WIERZCHOLSKI K., *Oil velocity and pressure distribution in short journal bearing under Rivlin Ericksen lubrication*, System Analysis Modeling and Simulations, OPA Overseas Publishers. Assoc. N.V., 1998, Vol. 32, 205–228.
[14] WIERZCHOLSKI K., *The method of solutions for hydrodynamic lubrication by synovial fluid flow in human joint gap*, Control and Cybernetics, 2002, Vol. 31, No. 1, 91–116.
[15] WIERZCHOLSKI K., *Capacity of deformed human hip joint gap in time dependent magnetic field*, Acta of Bioengineering and Biomechanics, 2003, Vol. 5, No. 1, 43–65.
[16] WIERZCHOLSKI K., *Pressure distribution in human joint gap for elastic cartilage and time dependent magnetic field*, Russian Journal of Biomechanics, Perm, 2003, Vol. 7, No. 1, 24–46.
[17] WIERZCHOLSKI K., *Tribologie für menschliche Gelenke*, Tribologie und Schmierungstechnik, 2002, 5, 5–13.
[18] WIERZCHOLSKI K., *Comparison between impulsive and periodic non-Newtonian lubrication of human hip joint*, Engineering Transactions, 2005, 53, 1, 69–114.
[19] WIERZCHOLSKI K., *Lubrication of deformed hip joint*, International Conference System Modelling and Control, Zakopane, 2007, 1–8.
[20] WIERZCHOLSKI K., MISZCZAK A., *Flow on the bio-cell surfaces as an element of the microbearing tribology*, Journal of Kones Powertrain and Transport, 2007, Vol. 14, No. 2, 553–560.
[21] WIERZCHOLSKI K., MISZCZAK A., *Load carrying capacity of microbearings with parabolic journal*, Solid State Phenomena, Trans. Technical Publications, Switzerland, 2009, Vol. 147–149, 542–547.
[22] WIERZCHOLSKI K., *Hydrodynamic pressure, carrying capacity, friction forces in biobearing gap*, Acta of Bioengineering and Biomechanics, 2009, Vol. 11, No. 2, 31–44.
[23] WIERZCHOLSKI K., *Friction force and pressure calculations for time dependet impulsive intelligent lubrication of human hip joint*, Acta of Bioengineering and Biomechanics, 2010, Vol. 12, No. 3, 95–101